GROUND DEFORMATION MEASUREMENTS OVER LAKE TRICHONIS BASED ON SAR INTERFEROMETRY

Benekos G.[1], Parcharidis I .[1], Foumelis M .[2] and Ganas A [3].

[1] Harokopio University of Athens, Department of Geography, El. Venizelou 70 Kallithea, 17671 Athens, Greece, parchar@hua.gr, benekos@hua.gr

[2] European Space Agency (ESA-ESRIN), Via Galilieo Galilei, 00044 Frascati, Italy, michael.foumelis@esa.int

[3] National Observatory of Athens, Geodynamic Institute, 11810 Athens, Greece, aganas@noa.gr

Abstract

The aim of this study is to detect and measure ground deformation over the broader area of Lake Trichonis (Western Greece), focusing mainly on the April 2007 earthquake swarm which occurred at the vicinity of the Lake. The area, forming a pull-apart basin, presented historically an intense seismic activity along the two active normal faults at the northern and southern part of the Lake. The swarm initiated by small magnitude events on the 8th of April 2007 followed by the three strongest events of the entire sequence on the 10th of April 2007, with magnitudes ranging from 5.0 to 5.2 Mw. The seismic activity continued for longer with smaller seismic events. Based on seismological data this activity was attributed to two unmapped NW SE trending normal faults that bounds the SE bank of the Lake. Using a dataset of 28 ENVISAT ASAR scenes covering the period from February 2003 until February 2010 (~7 yr), different Interferometric Stacking techniques was applied in order to quantify the ground deformation induced by the earthquake swarm as well as its effect on the inter-seismic deformation pattern of the area. Our results indicate that co-seismic motion differs significantly from that observed during the pre- and post- swarm periods. The co-seismic pattern reveals subsidence at the northern and uplift at the southern lake sides, consistent with the structural model already proposed for the area. For the pre- and post-seismic periods both sides of the Lake show stability or low rates of subsidence with higher deformation velocity rates for the period after the seismic activity, possibly attributed to post-seismic relaxation. Our findings imply that inter-seismic ground deformation does not necessary follow the deformation pattern observed during seismic triggering, thus, long-term geodetic observations such as those provided by SAR interferometry are valuable in order to fully characterize the geodynamic behavior of an active region.

Key words: SAR interferometry, ground deformation, earthquake swarm, Trichonis Lake, Greece

Περίληψη

Ο σκοπός της παρούσας μελέτης είναι ο εντοπισμός της παραμόρφωση του εδάφους στην ευρύτερη περιοχή της Λίμνης Τριχωνίδας (Δυτική Ελλάδα), εστιάζοντας κυρίως

στο σεισμικό φαινόμενο του Απριλίου 2007 με την σμήνοσειρά σεισμών που σημειώθηκε στην περιοχή της λίμνης. Η περιοχή συνιστά μία pull-apart λεκάνη, η οποία παρουσιάζει γενικότερα μία έντονη σεισμική δραστηριότητα λόγω των δύο ενεργών ρηγμάτων κατά μήκος του βόρειου και νότιου περιθωρίου της. Η σμήνοσειρά ξεκίνησε με μικρού μεγέθους σεισμούς, στις 9 Απριλίου 2007 ενώ ακλούθησαν τρία ισχυρότερα σεισμικά γεγονότα στις 10 Απριλίου 2007, με μεγέθη που κυμαίνονται από 5,0 έως 5,2 Mw, τα οποία και αποτέλεσαν τα μεγαλύτερα ολόκληρης της ακολουθίας. Η σεισμική δραστηριότητα συνεχίστηκε για περισσότερο από ένα μήνα με μικρότερα σεισμικά γεγονότα. Βάσει των σεισμολογικών δεδομένων οριοθετήθηκαν δύο νέα κανονικά ρήγματα ΒΔ-ΝΑ διεύθυνσης κατά μήκος της νοτιοανατολικής όχθης της λίμνης. Χρησιμοποιώντας ένα σύνολο 28 εικόνων Ραντάρ, του δορυφόρου ENVISAT για την περίοδο από το Φεβρουάριο του 2003 μέχρι τον Φεβρουάριο του 2010 εφαρμόστηκε η τεχνική της διαφορικής συμβολομετρίας και πιο συγκεκριμένα διαφορετικές τεχνικές σώρευσης συμβολογραφημάτων με σκοπό την ανίχνευση και χαρτογράφηση των παραμορφώσεων του εδάφους που προκλήθηκε από την «σμήνοσειρά σεισμών». Σύμφωνα με τα αποτελέσματά των συγκεκριμένων τεχνικών αποδεικνύεται ότι η περιοχή παρουσιάζει εντελώς διαφορετικό καθεστώς εδαφικής παραμόρφωση κατά τη διάρκεια της προ-σεισμικής και μετα-σεισμικής περίοδου σε σχέση με την συν-σεισμική.

Λέξεις κλειδιά:, Συμβολομετρία Ραντάρ, εδαφική παραμόρφωση, σμήνοσειρά, Λίμνη Τριχωνίδα, Ελλάς

1. Introduction

During the last two decades spaceborne Synthetic Aperture Radar (SAR) interferometry has become a useful geodetic tool for ground deformation detection and monitoring (Massonnet et al., 1993; Zebker et al., 1994; Galloway et al., 1998; Wright and Stow, 1999; Carnec and Fabriol, 1999; Strozzi et al., 2001; 2002; Foumelis et al., 2009).

The potentials of SAR interferometry has motivated many scientists to apply this technique for a wide range of applications related to seismo-tectonics. The utilization of an appropriate interferometric dataset allows measuring the various components of the seismic cycle, namely the pre-seismic, co-seismic, and post-seismic deformation (Massonnet et al., 1993; Peltzer et al., 1998; Peltzer and Crampé, 1999; Donnellan et al., 2002). Such analysis was performed in the present study to investigate the deformation caused by the April 2007 Trichonis's Lake Basin earthquake swarm as well as its effect on the inter-seismic pattern of the area.

The seismic sequence initiated by small events on the 8th of April 2007, while two days later, three of the strongest events in the whole sequence occurred (10th of April at 03:17, 07:15 and 10:41 GMT), with magnitudes ranging from 5.0 Mw to 5.2 Mw. The seismic activity continued for more than a month with smaller events (Sokos et al., 2010; Evangelidis et al., 2008; Kiratzi et al, 2008). The above studies provided insights on the activation of an unmapped NW–SE fault zone.

2. Geological Setting

Trichonis is the largest natural lake in Greece, covering an area of 97 km^2 and located in the western part of the country. On the northeastern side of the lake, there is the high slope of the Panaitoliko Mountain, whereas to the southwestern, the ridge of Arakintho Mountain (Figure 1). The broader Trichonis basin is a 30-km-long by 10-km-wide neo-tectonic graben (Doutsos et al., 1987). Its southern border is marked by a major WNW-ESE trending normal fault. The main geological formations belong to the External Hellenides, namely the Pindos and Gavrovo geotectonic units. The lake of Trichonis occupies the east edge of the fractured tectonic trough that retains a semi-circular shape. The formation of this trough is mainly due to the intense tectonism

of the area and partly to the falling down of limestone masses into the existing underground caverns, which form a quite extensive underground karstic network (Figure 2). The underground caverns of this network are being enlarged due to the erosive and solvent action of the water, resulting thus to the fall of the overlying layers and, finally, to the change of the morphology of the region (Evangelidis et al., 2008 and Kiratzi et al., 2008).
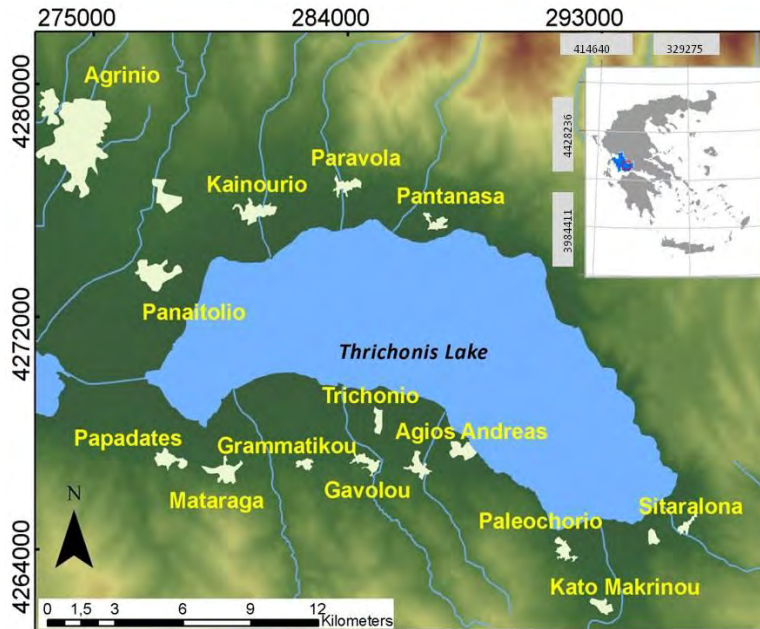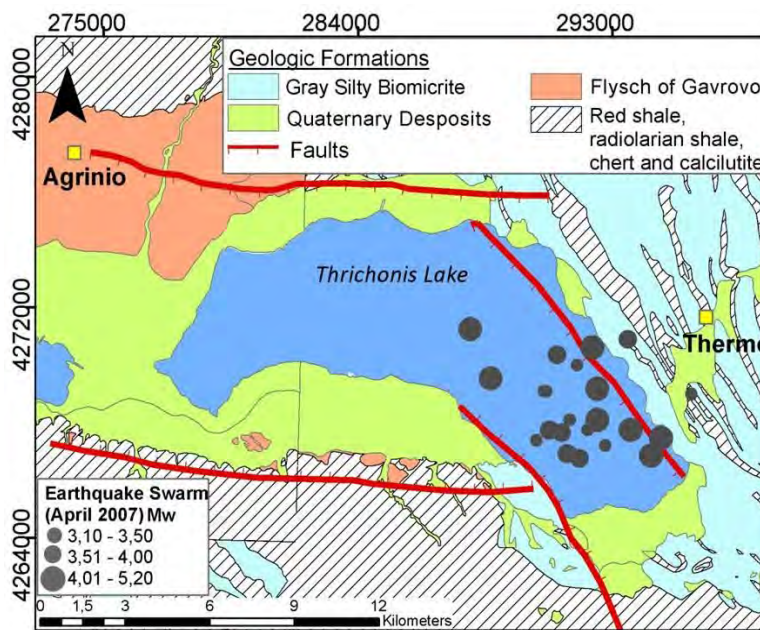

Figure 1 - Location map of the study area

Figure 2 - Simplified geological map of the broader study area (IGME 1977). Epicenters of the earthquake swarm of April 2007 are also shown (Kiratzi et al., 2008).

3. Geodynamic Regime

3.1. Tectonic Settings

The Trichonis graben is a well-known Quaternary structure that strikes WNW–ESE for a distance of about 32 km and has a width of about 10 km. The graben cuts across the Pindos Mountains and strikes almost parallel to the Gulf of Patras graben about 30 km to the south. The Trichonis Fault zone is the major, topography controlling north-dipping normal fault, which bounds the south shore of the lake where it is locally buried under Pleistocene deposits and thick alluvial cones (Doutsos et al., 1987). The fault forms a distinct topographic escarpment with clear drainage incision in the footwall block.

3.2 Seismicity

The majority of the seismic events in the area are well-constrained along the southeastern side of the lake. Historical records exist since 1841 for that region, illustrating an average yearly earthquake magnitude of 5 in the Mercalli-Sieberg scale until 1959 (Delibasis and Carydis, 1977). It should be mentioned that in 1975 from June to December there was a sequence of earthquakes in the southern part of the lake. The first of the largest earthquakes took place on 30 June 1975 (M 5.4) whereas on 21 December 1975 an M 5.1 event was followed by another on 31 December 1975 with a magnitude of 5.1 (Papazachos et al., 1997; Evangelidis et al., 2008; Kiratzi et al., 2008). Specifically, in the southeastern part of the lake a strong seismic activity with a series of relative strong earthquakes started in April 2007 (Figure 2). The swarm began with small events, on April 9 and two days later occurred the three strongest events of the entire sequence (10 April at 3:17, 07:15 and 10:41 GMT), with sizes ranging from 5.2 to 5.0 Mw (Table 1). The seismic activity continued for a month with smaller magnitude events (Evangelidis et al., 2008; Kiratzi et al., 2008). It was shown that this seismic activity does not correlate with any of the two fault zones at the northern and southern edges of the lake, but with two unmapped NNE-SSW and NW-SE faults along its eastern shore (Sokos et al., 2010; Evangelidis et al., 2008; Kiratzi et al., 2008). Also the seismic activity of 1975 associated with these normal faulting along a NNW–ESE striking fault, combined with a left lateral component of the slip vector. This strike-slip is linked with the vertical rotation axis of the cortex and the left fracture associated with fault zones, Trichonis and the Corinthian Gulf (Kiratzi et al., 2008 and Sokos et al., 2010).

4. Data Used and Methodology

For the scope of the study, a total number of 28 ENVISAT ASAR scenes acquired along the ascending track 279 and covering the period between 2003 and 2010 (~7 yr) (Table 2), were processed using the GAMMA software. Initial estimations of the interferometric baselines were calculated from the Deflt precise orbit state vectors (Scharoo and Visser, 1998). The topographic phase was simulated based on SRTM V3 DEM of approximate spatial resolution of 90 m.

Stacking of differential interferograms aims to combine the information from several observations, in order to extract common information (Sandwell and Sichoix, 2000; Parcharidis et al., 2006; Raucoules et al., 2008). The most straightforward procedure is to compute linear combinations by averaging of interferograms. Interferometric Stacking (IS) is useful in overcoming drawbacks of conventional Differential SAR Interfeometry (DInSAR) such as the temporal decorrelation while minimizing error sources related to atmospheric phase screen.

The main process steps followed comprise the co-registration of single look complex images (SLCs), simulation of the topographic phase , generation of differential interferograms, filtering, phase unwrapping, baseline refinement, and geocoding from SAR to map geometry. All possible interferometric combinations with baselines less than 150 m were computed resulting in a total number of 68 interferograms. These interferograms were filtered using an adaptive filtering

Table 1 - Epicenters of the 2007 earthquake (the strongest events of the swarm are marked with red), modified by (Kiratzi et al., 2008).

No	Year	Month	Day	h:min:s	Lat °N	Lon °E	Depth	Mw
1	2007	4	9	23:27:15.71	38,539	21,626	15,66	4,40
2	2007	4	10	00:54:56.35	38,529	21,629	14,91	3,40
3	2007	4	10	03:17:56.09	38,551	21,626	14,29	5,00
4	2007	4	10	03:27:38.33	38,534	21,612	5,28	3,90
5	2007	4	10	03:32:34.20	38,524	21,619	14,15	3,70
6	2007	4	10	03:39:18.86	38,549	21,663	12,49	3,30
7	2007	4	10	04:16:15.65	38,550	21,605	2,95	3,10
8	2007	4	10	04:29:58.11	38,535	21,607	10,96	3,70
9	2007	4	10	04:47:17.99	38,535	21,622	12,94	3,30
10	2007	4	10	05:55:12.15	38,531	21,602	9,70	3,10
11	2007	4	10	06:03:39.12	38,570	21,638	8,54	3,70
12	2007	4	10	07:13:03.67	38,532	21,651	14,60	4,70
13	2007	4	10	07:14:12.39	38,567	21,624	12,42	4,40
14	2007	4	10	07:15:40.44	38,555	21,584	5,06	5,10
15	2007	4	10	08:13:45.40	38,526	21,614	14,59	3,80
16	2007	4	10	09:59:01.51	38,560	21,618	11,63	3,50
17	2007	4	10	10:34:47.97	38,550	21,606	13,62	3,30
18	2007	4	10	10:41:00.14	38,525	21,647	22,47	5,20
19	2007	4	10	12:55:17.70	38,539	21,615	12,91	3,30
20	2007	4	10	13:51:00.93	38,564	21,610	17,81	3,60
21	2007	4	13	12:58:14.45	38,526	21,616	9,38	3,10
22	2007	4	15	02:16:32.58	38,574	21,576	17,86	4,10
23	2007	6	5	11:50:20.46	38,535	21,639	16,57	4,80

algorithm proposed by (Goldstein and Werner, 1998) to reduce phase noise. The levels of coherence, independently of the acquisition time intervals, were high only over build environment that reflects the villages around the lake. The majority of the arable areas around the lake exhibit significantly low coherence due to that don't reflected constant over time the signal. Subsequently, we reconstructed the unwrapped phase from the obtained differential interferograms, based on the assumption of the structured "phase unwrapping" rule; that is the phase difference between two neighbor pixels does not exceed the half cycle (π), and using the minimum cost network algorithm (Constantini, 1998).

Following phase unwrapping a baseline refinement procedure was adopted in order to more precisely define acquisition geometry and hence the simulation of topographic component. Finally, the unwrapped interferograms of the highest quality in terms of coherence levels was stacked in order to estimate ground deformation rates. In this step the selection of the reference points is considered to be one of the critical parts of the processing since it affects significantly the final deformation estimates. Some selection criteria are quantitative, such as the high coherence of the point in terms of phase stability overtime. Others are qualitative and are related to the regional tectonic setting of the area and the related pattern of deformation which needs to be extracted. The local reference point selected for the processing is located close to Agrinio town at the north-east part of the study area.

Also, a specific stacking strategy be followed, in order to develop two different time period IS processings. The first involves the pre-seismic period with 17 interferograms from the total 27 before the seismic swarm. The second one involves the post-seismic period with 9 from the 11

total interferograms. The selection of pairs is according to the criteria of quality as the residual phase and the noise in the unwrapped interferograms.

For the co-seismic period, there are no suitable interferometric pairs to follow the aforementioned IS procedure. In the case of non instantaneous (for example linear) deformation, summing interferograms on equivalent periods (approximately same start and end dates) partly reduce the atmosphere to deformation ratio and the obtained pseudo-interferograms will have an increased accuracy respect to initial ones. The sum of pairs covering successive periods was also computed to provide long time span pseudo-interferograms that could not be reliably covered by a single interferogram due to geometric (baseline) and temporal (coherence) limitations (Parcharidis et al., 2006). The linear combination in this case a sum of four interferograms covering the periods (i) 2007-01-16/2008-04-15, (ii) 2008-04-15/2008-09-02, and (iii) 2008-11-11/2009-12-20 resulted in the formation of a pseudo-interferogram spanning the period 2007–2009, where the co-seismic deformation signature of the earthquake swarm was identified.

Table 2 - List of ENVISAT ASAR.SLC dataset used in the analysis. Reference image in bold, Bp: perpendicular baseline and dT: temporal separation between acquisitions.

No	Master (Date)	Slave (Date)	Bp (m)	dT (days)
1	20050531	20030211	787	-840
2	20050531	20030805	-227	-665
3	20050531	20031014	38	-595
4	20050531	20031223	-439	-525
5	20050531	20040406	-69	-420
6	20050531	20040511	18	-385
7	20050531	20040720	-343	-315
8	20050531	20040824	340	-280
9	20050531	20040928	-683	-245
10	20050531	20041102	-551	-210
11	20050531	20050111	-494	-140
12	20050531	20050426	1001	-35
13	**20050531**	**20050531**	**0**	**0**
14	20050531	20060620	-656	385
15	20050531	20060725	1107	420
16	20050531	20061003	-587	490
17	20050531	20070116	375	595
18	20050531	20070220	-326	630
19	20050531	20080311	35	1015
20	20050531	20080415	308	1050
21	20050531	20080729	-269	1155
22	20050531	20080902	411	1190
23	20050531	20081007	-331	1225
24	20050531	20081111	156	1260
25	20050531	20090120	120	1330
26	20050531	20090224	-299	1365
27	20050531	20090505	-463	1435
28	20050531	20100209	138	1715

5. Results

By transforming the interferometric results from range–Doppler coordinates into map geometry, the interferometric analysis results were imported in a GIS environment for further interpretation. The obtained deformation maps for the pre-, co- and post-seismic periods are shown in (Figure 3).

The pre-seismic displacement field (Oct. 2003–Oct. 2006) shows relative stability, while locally low subsidence rates are observed. In the northern part of the lake subsidence prevails with the highest rate of -7 mm/yr in Paravola village. Similar deformation patterns are observed on the south side of the lake (up to -8 mm/yr). In the southeastern part of the lake, which should be considered separately because of the presence of the two active NW–SE fault zones, subsidence rates varies between -1 and -5 mm/yr (Figure 4).
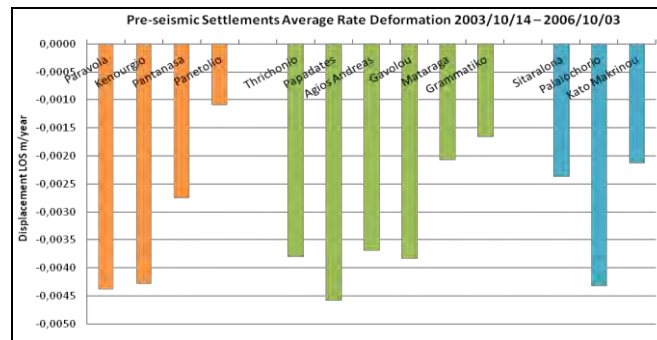

Figure 3 - Settlements' average deformation rates (along the Line-of-Sight - LOS) for the pre-seismic period, (Northern part – Orange columns, Southern part - Green columns, Southeast part - Blue columns).
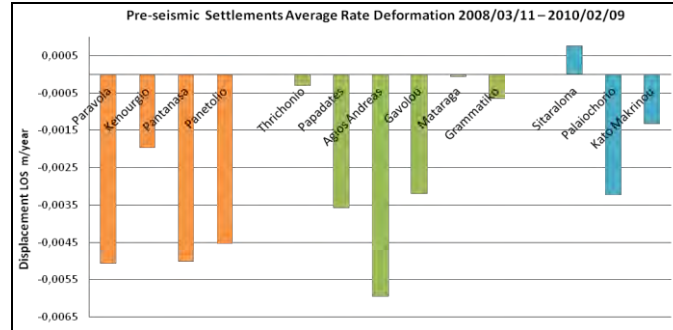

Figure 4 - Settlements' average deformation rates (in LOS) for the post-seismic period, (Northen part – Orange columns, Southern part - Green columns, Southeast part - Blue columns).

Moreover, the surface deformation is examined for the post-earthquake swarm period. Making a first reading in this post-seismic deformation map for the period Mar. 2008 – Febr. 2010, increased subsidence rates are observed compared to the pre-seismic results for the same areas. Specifically, the northern part of the Trichonis Lake subsides by up to -10.2 mm/yr. The southern part of the lake roughly follows the same pattern with rates up to 10 mm/yr. On the southeastern part of the lake, the Paleochori settlement subsides up to -1 mm/yr and Kato Makrinou shows subsidence until -8 mm/yr. But the Sitaralonona village shows mixed deformation patterns from 5 to -5 mm/yr (Figure 5).

The resulting pseudo-interferogramthat includes the effect of the earthquake swarm shows a different deformation pattern compared to the previously examined periods. The northern part of

the Trichonis' Lake shows subsidence patterns, on the contrary to the southern part where uplift is detected. This characteristic deformation pattern is also present on the southeastern part of the lake. This regions is examined separately because of two NW–SE faults resulting in uplifts at the western part while the eastern one shows significant subsidence rates (Figure 6).
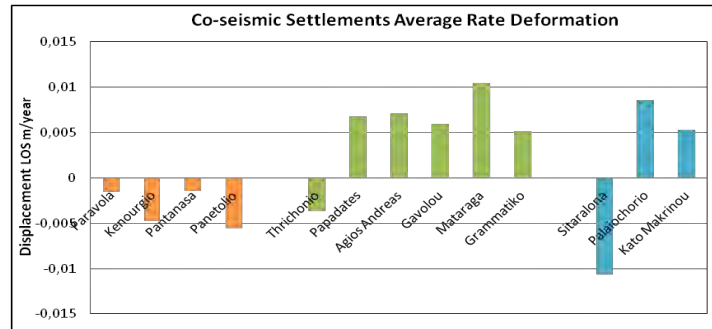

Figure 5 - Settlements' average deformation rates (in LOS) for the cot-seismic period, (Northen part – Orange columns, Southern part - Green columns, Southeast part - Blue columns)

6. Conclusion-Discussion

The IS technique was implemented to the Trichonis' lake area for the seismic event (earthquake swarm) on April 2007, showing the following results:

- The major subsidence rate in the post-seismic period compared to pre-seismic period. Probably the seismic event caused higher deformation velocities.

- This processing and the different deformation patterns in the displacement maps in the southeastern part of the lake verify the studies that promote the new tectonic settings that determined by the earthquake's swarm on April 2007 with two active faults in the southeastern part of the lake.

- Both the co- and inter-seismic displacement fields of the Trichonis Lake, the latter calculated for the periods before (2003-2006) and after (2007-2009) the swarm of earthquake in 2007, were investigated by means of SAR interferometric analysis.

  Regarding the co-seismic ground deformation, the adopted procedure to compensate for the lack of an appropriate single interferometric pair to cover the entire period of seismic activity, namely the linear combination of consecutive differential interferograms, led to the reduction of the error budget from possible atmospheric effects. Although this procedure provided acceptable results over build-up areas, the increase of the level of noise from individual pairs especially over agricultural and generally vegetated areas, which exhibit in turns high decorrelation, did not allowed deriving robust displacement observation.

- However, the relatively large number of villages in the region permitted the recognition of a characteristic co-seismic deformation pattern, with the entire northern part of the lake subsiding with an average rate of -5mm/yr, contrary to the southern part where uplift dominates by approximately 10mm/yr.

- Nonetheless, for an exact determination of the geometry of the activated fault zones as well as the amount of slip that took place, further modeling of the obtained InSAR results is necessary.

- As for the inter-seismic part, it was shown that the sign of motion is retained, though differences in the displacement rate do exist. Specifically, higher subsidence rates are

calculated for the post-seismic period, yet these differences lay within the uncertainty of the estimates and could be therefore neglected. It is worth to mention that no significant seismic activity was recorder during these periods.

- Finally, further analysis are required in order to identify and separate from the observed inter-seismic (pre- and post-) motion rates the effects of non-tectonic deformation-induced phenomena.
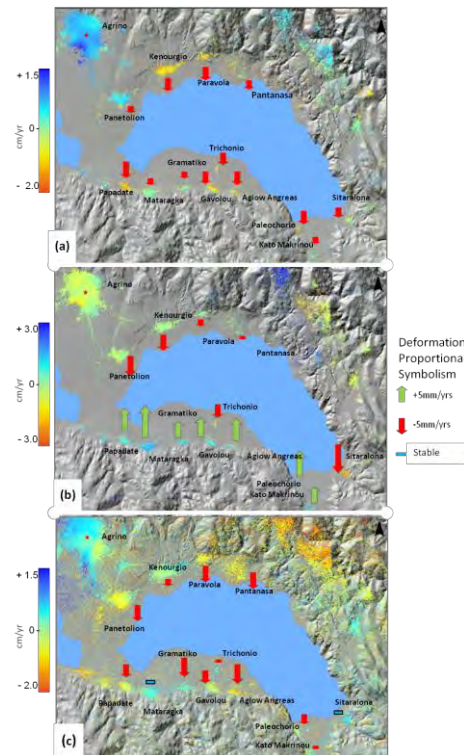

Figure 6 - Deformation rates maps of the broader area of Trichonis Lake by Interferometric Stacking for the (a) pre-seismic (2003-2006), (b) co-seismic (2007-2009) and (c) post-seismic (2008 -2009) periods. The red star represents the selected reference area.

7. Acknowledgments

8. References

Carnec C. and Fabriol H. 1999. Monitoring and modeling land subsidence at the Cerro-Prieto geothermal field, Baja California, Mexico, using SAR interferometry, *Geophys. Res. Lett. 9*, 1211–1214.

Costantini M. 1998. A novel phase unwrapping method based on network programming, 1998, *IEEE Trans. GARS*, 36 (3), 813 – 821.

Delibasis N. and Carydis P. 1977. Recent earthquake activity in Trichonis region and its tectonic significance, *Ann. Geofis.* 30, 19–81

Donnellan A., Parker and Peltzer G., 2002. Combined GPS and InSAR models of postseismic deformation from the Northridge earthquake, *Pure and Applied Geophysics* 159, 2261–2270.

Doutsos T., Kontopoulos N. and Frydas D. 1987. Neotectonic evolution of northwestern-continental Greece, *Geol. Rundsch*. 76, 433–450.

Evangelidis C.P., Konstantinou K.I., Melis N.S., Charalambakis M. and Stavrakakis G.N. 2008. Waveform relocation and focal mechanism analysis of an earthquake swarm in Trichonis lake, western Greece, *Bull. Seism. Soc. Am.* 98(2), pp. 804-811.

Foumelis M., Parcharidis I., Lagios E. and Voulgaris N. 2009. Evolution of post-seismic ground deformation of the Athens 1999 earthquake observed by SAR interferometry, *J. Appl. Geophys.* 69 (1), 16–23.

Galloway D.L., Hudnut K.W., Ingebritsen S.E., Phillips S.P., Peltzer G., Rogez F. and Rosen P.A. 1998. Detection of aquifer system compaction and land subsidence using interferometric synthetic aperture radar, Antelope Valley, Mojave Desert, California, *Water Resources Research*, 34 (10), pp. 2573-2585.

Goldstein R. and Werner C. 1998. Radar interferogram filtering for geophysical applications, *Geophys. Res. Lett*. 25 (21), 4035–4038.

IMGE 1977. Geological Map of Greece, Scale 1:50.000, Thermon Sheet, D.L. Loftus, N. Philippakis and A. Mavridis, The Institute of Geological and Minning Researche,

Kiratzi A., Sokos E., Ganas A., Tselentis A., Benetatos C., Roumelioti Z., Serpetsidaki A., Andriopoulos G., Galanis O. and Petrou P. 2008. The April 2007 earthquake swarm near Lake Trichonis and implications for active tectonics in western Greece, *Tectonophysics* 452, 51- 65.

Massonnet D. and Adragna F. 1993. A full-scale validation of Radar Interferometry with ERS-1: the Landers earthquake, Earth Observation Quarterly, 41.

Massonnet D., Rossi M., Carmona C., Adragna F., Pelmtzer G., Feigl K. and Rabaute T. 1993. The displacement field of the Landers Earthquake mapped by radar interferometry, *Nature* 364, 138–142.

Scharoo R. and Visser P.N.A.M. 1998. Precise orbit determination and gravity field improvement for the ERS satellites, *Journal Geophysical Research*, vol. 103, 8113-8127.

Papazachos B. and Papazachou K. 1997. The Earthquakes of Greece, Ziti Editions, Thessaloniki, Greece.

Parcharidis Is., Lagios E., Sakkas V., Raucoules D., Feurer D., Le Mouelic S., King C., Carnec C., Novali F., Ferretti A., Capes R. and Cooksley G. 2006, Subsidence monitoring within the Athens Basin (Greece) using space radar interferometric techniques, *Earth Planets Space*, 58, 505–513, 2006.

Peltzer G. and Crampé F. 1999. Evidence of non-linear elasticity of the crust from the Mw7.6 Manyi (Tibet) earthquake surface displacement field, *Science* 286 (5438), 272–276.

Peltzer G., Rosen P. and Rogez F. 1998. Poro-elastic rebound along the Landers 1992 earthquake surface rupture, *Journal of Geophysical Research B: Solid Earth 103 (B12), 30131–30145.*

Raucoules D., Parcharidis I., Feurer D., Novalli F., Ferretti A., Carnec C., Lagios E., Sakkas V., Le Mouelic S., Cooksley G. and Hosford S. 2008. Ground deformation detection of the greater area of Thessaloniki (Northern Greece) using radar interferometry techniques, *Natural Hazards Earth Syst. Sci. J.* 8 (4), 779–788.

Sokos E., Pikoulis V.E, Psarakis E.Z. and Lois A. 2010. THE APRIL 2007 SWARM IN TRICHONIS LAKE USING DATA FROM A MICROSEISMIC NETWORK, Bulletin of the Geological Society of Greece 2010, *Proceedings of the 12th International Congress* Patras May, XLIII, No 4 – 2183.

Strozzi T., Wegmuller U., Tosi L., Bitelli G. and Spreckels V. 2001. Land subsidence monitoring with differential SAR interferometry, *Photogramm. Eng. Remote Sens.* 67, 1261–1270.

Wright P., Stow, R., 1999. Detecting mining subsidence from Space, *Int. J. Remote Sens.* 20 (6), 1183–1188.

Zebker H.A., Rosen P.A., Goldstein R.M., Gabriel A. and Werner C.L. 1994. On the derivation of coseismic displacement-fields using differential radar interferometry: the Landers earthquake, *J. Geophys. Res. Solid Earth* 99 (B10), 19617–19634